

# Collinear approach for top quark production at the ep colliders

G.R.Boroun\*

Department of physics, Razi University, Kermanshah 67149, Iran

(Dated: October 12, 2021)

An analysis study of the collinear approach for  $t\bar{t}$  production at the Future Circular Collider hadron-electron (FCC-he) is performed. To study the heavy quark production processes, the collinear generalized double asymptotic scaling (DAS) approach at the next-to-next-to-leading order (NNLO) approximation at small Bjorken  $x$  values is used. Bounds on the top reduced cross section at the FCC-he center-of-mass energy and at the high inelasticity are derived. Expanding the method to high- values of  $Q^2$ ,  $Q^2 \geq m_t^2$ , can be considered in the process analysis of new colliders. A nonlinear modification of the evolution of the gluon density for heavy-quark production in DIS is obtained at small  $x$  from the parametrization of the proton structure function to include the effects of heavy-quark masses.

## I. Introduction

The Large Hadron electron Collider (LHeC) [1] and the Future Circular Collider hadron-electron (FCC-he) [2] are proposed facilities of using newly built electron-proton center of mass energies at  $\sqrt{s} \cong 1.3$  and 3.5 TeV, respectively. The electron beam 60 GeV collide with the intense hadron beams of the LHC. The LHeC and FCC-he measurements can be performed with much increased precision and extended to much lower values of  $x$  and high  $Q^2$ . These new colliders will be devoted to probing the energy frontier and complementing the discovery potential of the LHC with measurements of deep inelastic scattering (DIS). The LHeC and FCC-he collisions lead into the region of high parton densities at low  $x$  as the kinematic reach of maximum  $Q^2 \simeq 1$  TeV<sup>2</sup> and  $x \simeq 10^{-5..-6}$  for LHeC and  $10^{-7}$  for FCC-he. These kinematics are pertinent in investigations of lepton-hadron processes at ultra-high energy (UHE) neutrino astroparticle physics [3-4]. Moreover a similar very high energy electron-proton/ion collider (VHEep) [5] has been suggested based on plasma wakefield acceleration, albeit with very low luminosity. The center-of-mass energy, in this collider, is close to 10 TeV which is relevant in investigations of new strong interaction dynamics related to high-energy cosmic rays and gravitational physics. It can be used to study the top-quark physics [6-13]. In particular the LHeC and FCC-he will provide a cleaner environment for the study of top pair production. The top quark will produce in these future colliders in pairs ( $t\bar{t}$ ) through quantum chromodynamics (QCD) processes, mostly photon-gluon fusion (PGF) at ultra-high energies  $\gamma^* + g \rightarrow t + \bar{t}$ . The top quark is produced in nuclear collisions by gluon-gluon fusion (GGF) [14-17],  $g + g \rightarrow t + \bar{t}$ , at the LHC. The top quark pair production cross sections

are  $\sigma_{t\bar{t}} = 984.5$  pb at  $\sqrt{s} = 14$  TeV and  $\sigma_{t\bar{t}} = 826.4$  pb at  $\sqrt{s} = 13$  TeV at CMS [18] and ATLAS [19]. Top quark pair production at the LHC is thereby characterized by final states comprising the decay products of the two  $W$  bosons, and two  $b$  jets, where the  $\sigma_{tot}^{t\bar{t}}$  at ultra-high energies for  $\mu = m_t$  can be written [15]

$$\hat{\sigma}_{gg}(\beta, m_t) = \frac{\alpha_s^2}{m_t^2} \{ f_{gg}^{(0)} + \alpha_s f_{gg}^{(1)} + \alpha_s^2 f_{gg}^{(2)} + \mathcal{O}\alpha_s^3 \}. \quad (1)$$

The functions  $f_{gg}$  are known at leading and high-order approximations and depend only on dimensionless parameters  $\beta$  and  $\rho$ , where  $\beta^2 = 1 - \rho$  with  $\rho = 4m_t^2/s$  is the squared relative velocity of the final state top quarks having pole mass  $m_t$  and produced at the square of the gluonic center of mass energy  $s$ .

The total cross section for the single top quark production via charged current (CC) DIS scattering at the LHeC is 1.89 pb [1] due to the center-of-mass energy of 1.3 TeV and at the FCC-he is 15.3 pb [2] due to the center-of-mass energy of 3.5 TeV. It is 0.05 pb [1] for top quark pair production in  $t\bar{t}$  photoproduction mode at the LHeC and 1.14 pb at the FCC-he [2]. Its means that the top quark with mass about  $172.5 \pm 0.5$  GeV, which measured by ATLAS [19] and CMS [18], and particle that most strongly influences the Higgs boson and its potential is special among all quarks, can be consider at future colliders. The observed effects of the  $t\bar{t}$  productions at the LHC are implemented on the CT18 PDFs recently in [20].

In the future circular colliders, top quark pair production via NC ep scattering is dominant in all the top quark production channels. I can utilize this unprecedented facility to measure the precise properties of the top quark and search for new physics.

In this work the collinear approach calculation of the top quark pair production at the FCC-he kinematic region is presented. I focus on the reduced cross section of the top quark. The parametrization of gluon distribution due to the number of active flavour in this calculation is

---

\*Electronic address: grboroun@gmail.com; boroun@razi.ac.ir

included. The rest of this paper is organized as follows. In Sec. II, theoretical framework for the coefficient function in collinear approach is presented. In Sec. III, the numerical results for the reduced cross section  $\sigma_r^{t\bar{t}}(x, Q^2)$  and for the deep inelastic structure function  $F_2^{t\bar{t}}(x, Q^2)$  at ultra-high energy processes are studied.

## II. Theory

The first production of heavy quarks at HERA is keeping by fixed number of parton densities (fixed flavour number schemes, FFNS) close to threshold  $\mu^2 \sim m^2$  (where  $m$  is the heavy quark mass). The resummation of collinear logarithms  $\ln(\mu^2/m^2)$  at scales far above the threshold  $\mu^2 \gg m^2$  is achieved through the use of variable flavour number schemes (VFNS). When the scale is increased above heavy quark mass thresholds, the number of active flavors increases in VFNS. For realistic kinematics it has to be extended to the case of a general-mass VFNS (GM-VFNS) which is defined similarly to the zero-mass VFNS (ZM-VFNS) in the  $Q^2/m^2 \rightarrow \infty$  limit [21,22]. In GM-VFNS the transition from  $n_f$  active flavors to  $n_f+1$  considered in the construction of charm-quark parton distribution function. Rather at some large scales the transition with two massive quarks (i.e.,  $n_f \rightarrow n_f+2$ ) has been discussed in Refs.[23,24]. The LHeC provides data on the charm and bottom structure functions extending over nearly 5 and 6 orders of magnitude in  $x, Q^2$ , respectively [1].

Recently in Ref.[25] authors studied the heavy quark production processes by the transverse momentum dependent (TMD) gluon distribution function. They used the Kimber-Martin-Ryskin [26] prescription from the Bessel-inspired behavior of parton densities at small  $x$ . The heavy quark reduced cross-section is defined in terms of the heavy quark structure functions as

$$\sigma_r^{Q\bar{Q}}(x, Q^2) = F_2^{Q\bar{Q}}(x, Q^2) - f(y)F_L^{Q\bar{Q}}(x, Q^2), \quad (2)$$

where  $f(y) = y^2/1 + (1-y)^2$  and  $y$  is the inelasticity. In the collinear generalized double asymptotic scaling (DAS) [27] approach, the heavy quark structure functions are driven at small  $x$  by gluons as

$$F_k^{Q\bar{Q}}(x, Q^2) = C_{k,g}^{Q\bar{Q}}(x, Q^2, m_Q^2) \otimes G(x, Q^2), \quad (k = 2, L). \quad (3)$$

The  $\otimes$  symbol denotes the convolution integral which turns into a simple multiplication in Mellin  $N$ -space and the notation is given by  $a(x) \otimes b(x) = \int_x^1 \frac{dz}{z} a(z)b(\frac{x}{z})$  and  $G(x, Q^2)$  is the gluon distribution function. The coefficient functions until the next-to-next-to leading order (NNLO) approximation [25] read

$$C_{k,g}(x, Q^2) = e_Q^2 a_s(\mu^2) [B_{k,g}^{(0)}(x, a) + a_s(\mu^2) B_{k,g}^{(1)}(x, a) + a_s^2(\mu^2) B_{k,g}^{(2)}(x, a)], \quad (4)$$

where  $a = m^2/Q^2$  and  $a_s(\mu^2) = \alpha_s(\mu^2)/4\pi$ . The explicit expression for the coefficient function is relegated in Appendix A. The default renormalisation and factorization scales are set to be equal  $\mu_R^2 = Q^2 + 4m^2$  and  $\mu_F^2 = Q^2$ . In order to fix the unphysical mass scale  $\mu$ , the renormalisation and factorisation scale for the heavy quarks is set to  $\mu^2 = Q^2 + 4m^2$ .

In the GM-VFNS at high  $Q^2$ , the heavy-flavor structure functions are dependence to the active flavor number as I take  $n_f = 4$  for  $m_c^2 < \mu^2 < m_b^2$ ,  $n_f = 5$  for  $m_b^2 < \mu^2 < m_t^2$  and  $n_f = 6$  for  $\mu^2 \geq m_t^2$ . Within this scheme, deep inelastic scattering measurements at the FCC-he and the LHeC will allow the top quark production via the  $g \rightarrow Q\bar{Q}$  evolution. In the small- $x$  range the top quark contributions are given by the following form

$$F_k^{t\bar{t}}(x, Q^2) = C_{k,g}^{t\bar{t}}(x, Q^2, m_t^2) \otimes G_{n_f=6}(x, Q^2), \quad (5)$$

where  $G_{n_f}$  is the gluon distribution function due to the number of active quark flavors.

In the present of heavy quarks, the gluon distribution functions  $G_{n_f}(x, Q^2)$  defined to take into account the effect the production thresholds for pairs of heavy quarks. In Ref.[28] authors have been uses from a simplified version of the method introduced by Aivazis, Collins, Olness, and Tung (ACOT) [29] by a scaling variable  $x_i = x[1 + 4M_i^2/Q^2]$  where  $i \in u, \bar{u}, d, \bar{d}, s, \bar{s}, c, \bar{c}, b, \bar{b}$ . Authors [28] shown that the gluon distribution is defined with respect to treat mass effects as

$$G_{n_f=4}(x, Q^2) = \frac{3}{5} G_{n_f=3}(x, Q^2), \quad (6)$$

and

$$G_{n_f=5}(x, Q^2) = \frac{6}{11} G_{n_f=3}(x, Q^2). \quad (7)$$

$G_{n_f=3}(x, Q^2)$  is dependent on  $F_2(x, Q^2)$  and  $\partial F_2(x, Q^2)/\partial \ln x$  using a Laplace transform method. The proton structure function  $F_2(x, Q^2)$  parameterized with a global fit to the ZEUS data for  $x < 0.1$ . Several methods for the determination of the charm and bottom quark structure functions in the nucleon have been proposed in Refs.[30-33].

More generally, in comparison with the three massless quarks ( $n_f = 3$ ), I define the ratio of gluon distributions  $\frac{G_{n_f+j}}{G_{n_f}}|_{j=1-3}$  with respect to the effect of production thresholds for pairs of heavy quarks by the factor  $\frac{\sum_i^{n_f} e_i^2}{\sum_i^{n_f+j} e_i^2}|_{j=1-3}$ . Thus, the gluon distribution function for 6 quarks at  $Q^2 \geq m_t^2$  is obtained into the three massless quarks gluon distribution function,  $G_{n_f=3}$ , by the factor  $[6/9]/[15/9]$  as

$$G_{n_f=6} = \frac{2}{5} G_{n_f=3}. \quad (8)$$

Therefore

$$\sigma_r^{t\bar{t}}(x, Q^2) = [C_{2,g}^{t\bar{t}}(x, Q^2, m_t^2) - f(y)C_{L,g}^{t\bar{t}}(x, Q^2, m_t^2)] \otimes G_{n_f=6}(x, Q^2). \quad (9)$$

With the explicit form of the coefficient functions, I can proceed to extract the top reduced cross section  $\sigma_r^{t\bar{t}}(x, Q^2)$  from the parametrization of  $G_{n_f}(x, Q^2)$  for  $Q^2 \geq m_t^2$  at the collinear approach.

In order to make sure these results are in the deep inelastic region, the nonlinear corrections to the gluon distribution are taken into account. It is known that the absorptive corrections (or gluon recombination effects) in the low  $x$ , low  $Q^2$  region are not negligible and reduce the growth of the gluon parton distribution function. For small momentum transfer the produced gluon overlap themselves in the transverse area and fusion processes,  $gg \rightarrow g$ , become important [34-40]. The theoretical predictions of these effects were first emphasized long ago by Gribov, Levin and Ryskin [41] and followed by Mueller and Qiu (MQ) [42].

The evolution of the gluon density is modified at low values of  $x$  by an extra non-linear term, quadratic in the gluon density, as

$$\frac{\partial G(x, Q^2)}{\partial \ln Q^2} = \frac{\alpha_s(Q^2)}{2\pi} P_{gg} \otimes G(x, Q^2) - \frac{81 \alpha_s^2(Q^2)}{16 \mathcal{R}^2 Q^2} \int_\chi^1 \frac{dz}{z} G^2\left(\frac{x}{z}, Q^2\right), \quad (10)$$

where  $\chi = \frac{x}{x_0}$  and  $x_0$  is the boundary condition that the gluon distribution joints smoothly onto the linear region. The correlation length  $\mathcal{R}$  determines the size of the nonlinear terms, as  $\mathcal{R} \sim 1$  is of the order of the proton radius. Eq.(10) leads to saturation of the gluon density at low  $Q^2$  with decreasing  $x$ . To investigate the role of the non-linear effects on the behavior of the heavy quark distribution functions in the low  $x$  region, I first correct the low  $x$  non-linear gluon density behavior using the known saturation effects. This effect plays the role of a non-linear correction, which nevertheless may be important in describing the top reduced cross section data at the LHeC and FCC-he colliders.

### III. Results and Discussions

In this analysis, the value of  $\alpha_s(M_z)$  is set to the world average of  $\alpha_s(M_z) = 0.118$ , in line with the recommended value from the particle data group (PDG) [43]. In accordance with the values recommended by the Higgs Cross Section Working Group [44], the charm-quark, bottom-quark and top-quark pole masses are set as in the NNPDF default analysis to  $m_c = 1.65$  GeV and  $m_b = 4.78$  GeV and  $m_t = 172.5$  GeV [45] respectively.

In Fig.1, the behavior of the top-quark reduced cross section, with respect to the number of active flavor  $n_f = 6$ , for  $Q^2 \geq m_t^2$  at center-of-mass energy  $\sqrt{s} = 3.5$  TeV is considered. The top reduced cross section in electron-proton collision at FCC-he can provide a stringent test of new physics at UHE. To show the contribution and importance of the longitudinal structure function  $F_L^t(x, Q^2)$ , I derive bounds on the top reduced cross section at high-inelasticity  $y = 1$ , as

$$\begin{aligned} \sigma_r^{t\bar{t}}(x, Q^2) &= F_2^{t\bar{t}}(x, Q^2) - F_L^{t\bar{t}}(x, Q^2), \\ &= [C_{2,g}^{t\bar{t}}(x, Q^2, m_t^2) - C_{L,g}^{t\bar{t}}(x, Q^2, m_t^2)] \\ &\quad \otimes G_{n_f=6}(x, Q^2). \end{aligned} \quad (11)$$

Notice that the large inelasticity is only for scattered electron energies much smaller than the electron beam energy, where the electromagnetic and hadronic backgrounds are important. Eq.(11) is an upper bound on the top reduced cross section at UHE. It is shown that this bound can be used to constrain the range of applicability of the linear and non-linear corrections to the top reduced cross section at FCC-he collider. The non-linear corrections increase the top reduced cross section as  $Q^2$  increases. The nonlinear effects of the top reduced cross section are observable at hotspot point, where the value of this parameter is defined to be  $R = 2$  GeV<sup>-1</sup>. In Fig.1 we observe that the maximum value for the top reduced cross section is obtained at  $Q^2 \simeq 5m_t^2$ .

Importance of top quark longitudinal structure function measurements [46] at future circular collider energies are considered in Fig.2. The difference between the estimated  $\sigma_r^{t\bar{t}}$  and  $F_2^{t\bar{t}}$  is coming from the contribution of the longitudinal structure function  $F_L^{t\bar{t}}$ . So, these calculations show that these contributions are rather important at high  $Q^2$ . Numerical results for the ratio  $F_2^{t\bar{t}}/\sigma_r^{t\bar{t}}$  are shown in Fig. 2. This ratio calculated in the linear and non-linear corrections in a wide range of  $x$  values.

Results of these calculations for  $R^{t\bar{t}}$  are presented in Fig.3. The ratio  $R^{t\bar{t}} = F_L^{t\bar{t}}/F_2^{t\bar{t}}$  is plotted as a function of  $Q^2$  in a wide  $Q^2$  range. The maximum value for the ratio  $R^{t\bar{t}}$  is equal to  $\simeq 0.16$  over a wide range of  $Q^2$  values at NNLO approximation. For  $Q^2 > 5m_t^2$ , the ratio decrease as  $Q^2$  increases. Indeed, the asymptotic large- $Q^2$  dependence of  $R^{t\bar{t}}$  at NNLO should be proportional to  $\alpha_s^2(Q^2)$  and thus decreasing. The maximum value of the ratio  $R^{t\bar{t}}$  is almost constant [30] on the energy shift from HERA to the FCC-he. Consequently, the linear and non-linear corrections make it possible to perform the high-order corrections to the ultra-high-energy processes in heavy quark production due to the rescaling variable.

To summarize, I used the collinear approach to obtain the heavy-quark structure functions at small Bjorken  $x$  values at NNLO approximation. The method presents

an application of extraction of the gluon density due to the number of active flavor. With respect to the parameterization of  $F_2$ , the gluon density gives an excellent approximation behavior using a simplified ACOT approximation when the heavy-quarks are properly treated as massive. The non-linear corrections to the heavy-quark production of gluon density at small  $x$  at hot-spot point are implemented as improved the heavy-quark structure functions in comparison with the experimental data and the parameterization models. Starting with  $Q^2 \geq m_t^2$ , the collinear approach leads to important values for the top reduced cross section at the FCC-he collider, that needs an future investigations. For top quark pair production, which will be an important production channel at both LHeC and FCC-eh, the linear and non-linear reduced cross sections were determined. The results of the top reduced cross section are available with respect to the high inelasticity, defined in accordance with the center-of-mass energy. This method has derived bounds on  $\sigma_r^{t\bar{t}}$  from the collinear approach at the NNLO approximation due to the FCC-he center-of-mass energy. Also the importance of the longitudinal structure function measurements at future circular collider energies for top-quark production in the ratios  $F_2^{t\bar{t}}/\sigma_r^{t\bar{t}}$  and  $F_L^{t\bar{t}}/F_2^{t\bar{t}}$  were considered. The ratio of top structure functions were studied at NNLO approximation with take into account the top quark mass in the rescaling variable, which is proposed for the FCC-he. This study of the  $t\bar{t}$  threshold will be performed for the FCC-he collider.

## ACKNOWLEDGMENTS

The author is thankful to the Razi University for financial support of this project. The author was especially grateful to M. Klein and C.Schwanenberger for carefully reading the paper.

## APPENDIX A

In the high energy regime, defined by  $x \ll 1$ , the coefficient functions have the compact forms [25]

$$B_{k,g}^{(2)}(x, a) = \beta \ln(1/x) [R_{k,g}^{(2)}(1, a) + 4C_A R_{k,g}^{(1)}(1, a) L_\mu + 8C_A^2 B_{k,g}^{(0)}(1, a) L_\mu^2], \quad (12)$$

with

$$\begin{aligned} R_{2,g}^{(2)}(1, a) &= \frac{32}{27} C_A^2 [46 + (71 - 92a)J(a) \\ &\quad + 3(13 - 10a)I(a) - 9(1 - a)K(a)], \\ R_{L,g}^{(2)}(1, a) &= \frac{64}{27} C_A^2 x_2 \{34 + 240a - [3 + 136a + 480a^2]J(a) \\ &\quad + 3[3 + 4a(1 - 6a)]I(a) + 18a(1 + 3a)K(a)\}, \\ R_{2,g}^{(1)}(1, a) &= \frac{8}{9} C_A [5 + (13 - 10a)J(a) \\ &\quad + 6(1 - a)I(a)], \\ R_{L,g}^{(1)}(1, a) &= -\frac{16}{9} C_A x_2 \{1 - 12a - [3 + 4a(1 - 6a)]J(a) \\ &\quad + 12a[1 + 3a]I(a)\}, \\ B_{2,g}^{(0)}(1, a) &= \frac{2}{3} [1 + 2(1 - a)J(a)], \\ B_{L,g}^{(0)}(1, a) &= \frac{4}{3} x_2 \{1 + 6a - 4a[1 + 3a]J(a)\}, \end{aligned} \quad (13)$$

where

$$\begin{aligned} K(a) &= -\sqrt{x_2} [4(\zeta_3 + \text{Li}_3(-t) - \text{Li}_2(-t)\ln t \\ &\quad - 2S_{1,2}(-t)) + 2\ln(ax_2)(\zeta_2 + 2\text{Li}_2(-t)) \\ &\quad - \frac{1}{3}\ln^3 t - \ln^2(ax_2)\ln t + \ln(ax_2)\ln^2 t], \\ I(a) &= -\sqrt{x_2} [\zeta_2 + \frac{1}{2}\ln^2 t - \ln(ax_2)\ln t + 2\text{Li}_2(-t)], \\ J(a) &= -\sqrt{x_2} \ln t, \\ t &= \frac{1 - \sqrt{x_2}}{1 + \sqrt{x_2}}, \\ x_2 &= \frac{1}{1 + 4a}, \\ L_\mu &= \ln \frac{4m^2}{\mu^2}, \end{aligned} \quad (14)$$

where

$$\begin{aligned} \text{Li}_2(x) &= -\int_0^1 \frac{dy}{y} \ln(1 - xy), \\ \text{Li}_3(x) &= -\int_0^1 \frac{dy}{y} \ln(y) \ln(1 - xy), \\ S_{1,2}(x) &= \frac{1}{2} \int_0^1 \frac{dy}{y} \ln^2(1 - xy), \end{aligned} \quad (15)$$

are the dilogarithmic function  $\text{Li}_2(x)$ , the trilogarithmic function  $\text{Li}_3(x)$  and Nilsen Polylogarithm  $S_{1,2}(x)$ .

## References

1. P.Agostini et al. [LHeC Collaboration and FCC-he Study Group ], CERN-ACC-Note-2020-0002, arXiv:2007.14491 [hep-ex] (2020).
2. A. Abada et al., [FCC Collaboration], Eur.Phys.J.C **79**, 474 (2019).
3. M.Klein, arXiv:1802.04317; Annalen Phys. **528**, 138(2016).
4. R.A.Khalek et al., SciPost Phys.**7**, 051(2019).
5. A. Caldwell and M. Wing, Eur. Phys. J. C **76**, 463 (2016); A. Caldwell, et al., arXiv:1812.08110.
6. G. R. Boroun, ; Phys.Lett.B **744**, 142 (2015); Phys.Lett.B **741**, 197 (2015); Physics of Particles and Nuclei Letters **15**, 387(2018); Chin.Phys. C **41**, 013104 (2017).
7. I. A. Sarmiento-Alvarado, A. O. Bouzas, and F. Larios, J. Phys. G **42**, 085001 (2015).
8. Turk Cakir, A. Yilmaz, H. Denizli, A. Senol, H. Karadeniz, and O. Cakir, Adv. High Energy Phys.**2017**, 1572053 (2017).
9. H. Sun (LHeC/FCC-eh top physics Study Group), PoS DIS2018, 186 (2018).
10. C. Schwanenberger, PoS EPS-HEP2019, 635 (2020).
11. W. Liu and H. Sun, Phys. Rev. D **100**, 015011 (2019).
11. B. Yang, B. Hou, H. Zhang, and N. Liu, Phys. Rev. D **99**, 095002 (2019).
11. B. Rezaei and G. R. Boroun, EPL **130**, 51002 (2020).
12. H.Khanpour, Nucl.Phys.B **958**, 115141 (2020).
13. G.R.Boroun and B.Rezaei, EPL **133**, 61002 (2021).
14. M.Gao and J.Gao, arXiv:2103.15846.
15. V.A.Okorokov, J. Phys.: Conf. Ser. **1690**, 012006, (2020), arXiv:2010.03912.
16. O.B.Bylund, arXiv:2103.14772.
17. E.R.Nocera, M.Ubiali and C.Voisey, JHEP **05**, 067 (2020).
18. CMS Collaboration, Eur.Phys.J.C **79**, 368 (2019); Phys. Rev. D **93**, 072004 (2016).
19. ATLAS Collaboration, Phys. Lett. B **810**, 135797(2020); Eur. Phys. J. C **79**, 290 (2019).
20. Tie-Jiun Hou et al., Phys.Rev.D**103**, 014013(2021).
21. R.S.Thorne, arXiv:hep-ph/9805298(1998).
22. A.D.Martin W.J.Stirling and R.S.Thorne, Phys.Lett.B **636**, 259(2006).
23. J.Blümlein, A.De Freitas, C.Schneider and K.Schönwald, Phys. Lett.B **782**, 362(2018).
24. S.Alekhin, J. Blümlein and S. Moch, Phys. Rev. D **102**, 054014 (2020).
25. A.V.Kotikov, A.V.Lipatov and P.Zhang, arXiv:2104.13462 (2021).
26. M.A. Kimber, A.D. Martin, M.G. Ryskin, Phys. Rev. D **63**, 114027 (2001); G. Watt, A.D. Martin, M.G. Ryskin, Eur. Phys. J. C **31**, 73 (2003).
27. A.V. Kotikov, G. Parente, Nucl. Phys. B **549**, 242 (1999); A.Yu. Illarionov, A.V. Kotikov, G. Parente, Phys. Part. Nucl. **39**, 307 (2008); L. Mankiewicz, A. Saalfeld, T. Weigl, Phys. Lett. B **393**, 175 (1997).
28. M.M.Block and L.Durand, arXiv: 0902.0372 [hep-ph](2009).
29. M.A.G.Aivazis, J.C.Collins, F.I.Olness and W.-K.Tung, Phys.Rev.D **50**, 3102 (1994).
30. A.Y.Illarionov, B.A.Kniehl and A.V.Kotikov, Phys.Lett.B **663**, 66 (2008); A.Y.Illarionov and A.V.Kotikov, Phys.Atom.Nucl **75**, 1234 (2012).
31. G.R.Boroun and B.Rezaei, Int.J.Mod.Phys.E **24**, 1550063(2015); Nucl.Phys.A **929**, 119(2014); EPL **100**, 41001(2012); J.Exp.Theor.Phys. **115**, 427(2012); Nucl.Phys.B **857**, 143(2012)
32. J.Lan et al., arXiv [nucl-th]:1911.11676 (2019); N.N.Nikolaev and V.R.Zoller, Phys.Atom.Nucl. **73**, 672(2010); A. V. Kotikov, A. V. Lipatov, G. Parente and N. P. Zotov, Eur. Phys. J. C **26**, 51 (2002).
33. G.R.Boroun, Nucl.Phys.B **884**, 684(2014).
34. A.V.Giannini and F.O.Durães, Phys.Rev.D **88**, 114004(2013).
35. G.R.Boroun and B.Rezaei, arXiv [hep-ph]:2105.01121 (2021).
36. R.Wang and X.Chen, Chinese Phys.C **41**, 053103(2017).
37. G.R.Boroun and S.Zarrin, Eur.Phys.J.Plus **128**, 119(2013).
37. B.Rezaei and G.R.Boroun, Phys.Lett.B **692**, 247(2010).
39. D. Britzger, C. Ewerz, S. Glazov, O. Nachtmann, and S. Schmitt, Phys. Rev. D **100**, 114007 (2019).
40. G.R.Boroun, Eur.Phys.J.A **42**, 251(2009); Eur.Phys.J.A **43**, 335(2010)
41. L. V. Gribov, E. M. Levin and M. G. Ryskin, Phys. Rep. **100**, 1 (1983).
42. A. H. Mueller and Jianwei Qiu, Nucl. Phys. B **268**, 427 (1986).
43. PARTICLE DATA GROUP collaboration, *Review of particle physics*, Phys.Rev.D **98**, 030001 (2018).
44. LHC Higgs Cross Section Working Group collaboration, arXiv:1610.07922.
45. NNPDF Collaboration (Ball R. D. et al.), Eur. Phys. J. C **77**, 663 (2017).
46. G. R. Boroun, Chin. Phys. C **45**, 063105 (2021).

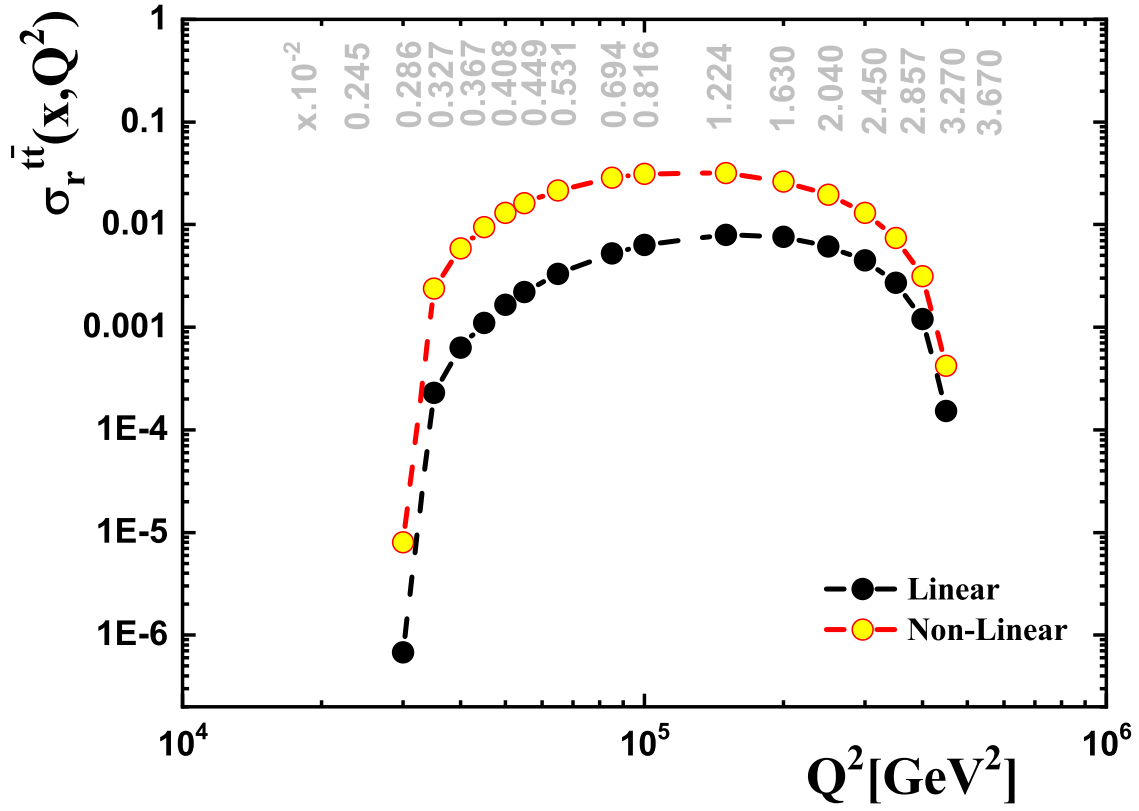


FIG. 1: The reduced top cross sections  $\bar{\sigma}_r^{t\bar{t}}(x, Q^2)$  as a function of  $x$  calculated at different  $Q^2$  values. The predictions obtained with analytical parameterization of the gluon density in a proton and collinear approach at NNLO approximation. The non-linear corrections to the reduced cross section are defined at hot-spot point. These values represent the contributions from the high inelasticity, as it is described in the text.

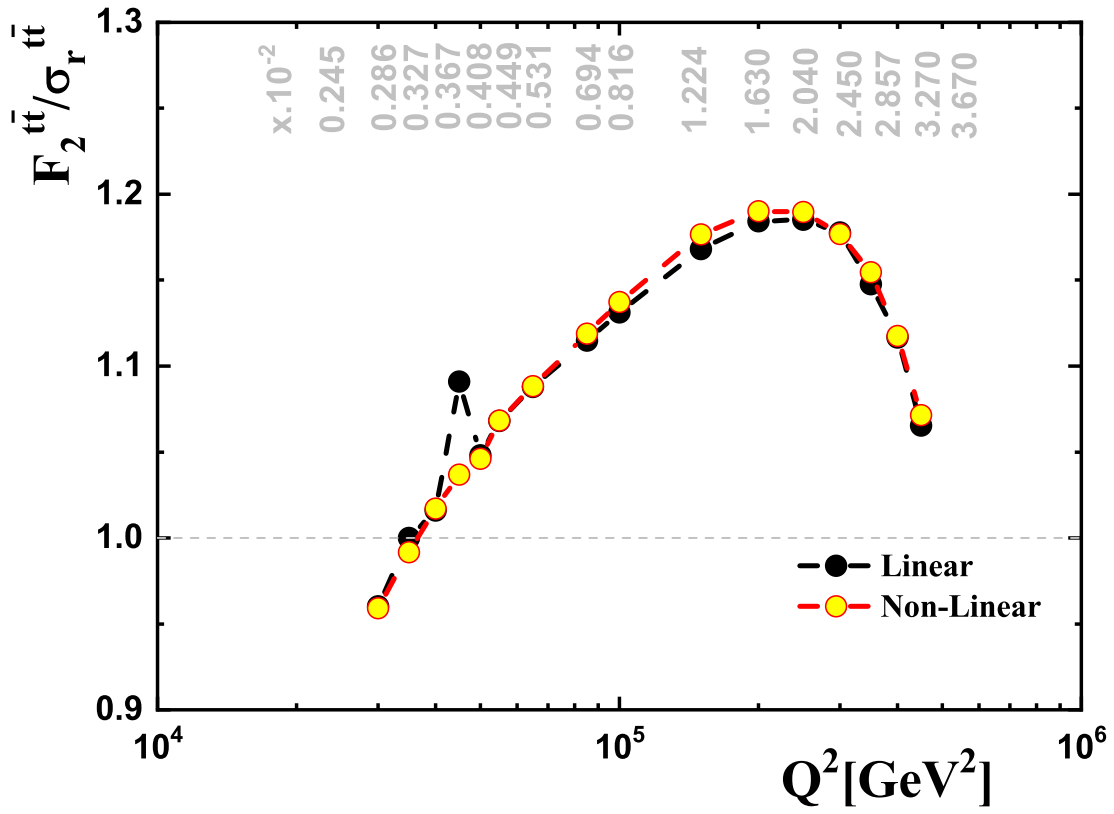


FIG. 2: The ratio  $F_2^{t\bar{t}}/\sigma_r^{t\bar{t}}$  are shown importance of top quark longitudinal structure function measurements at  $Q^2 \geq m_t^2$ . The non-linear corrections at hot-spot point are compared with linear in this figure.

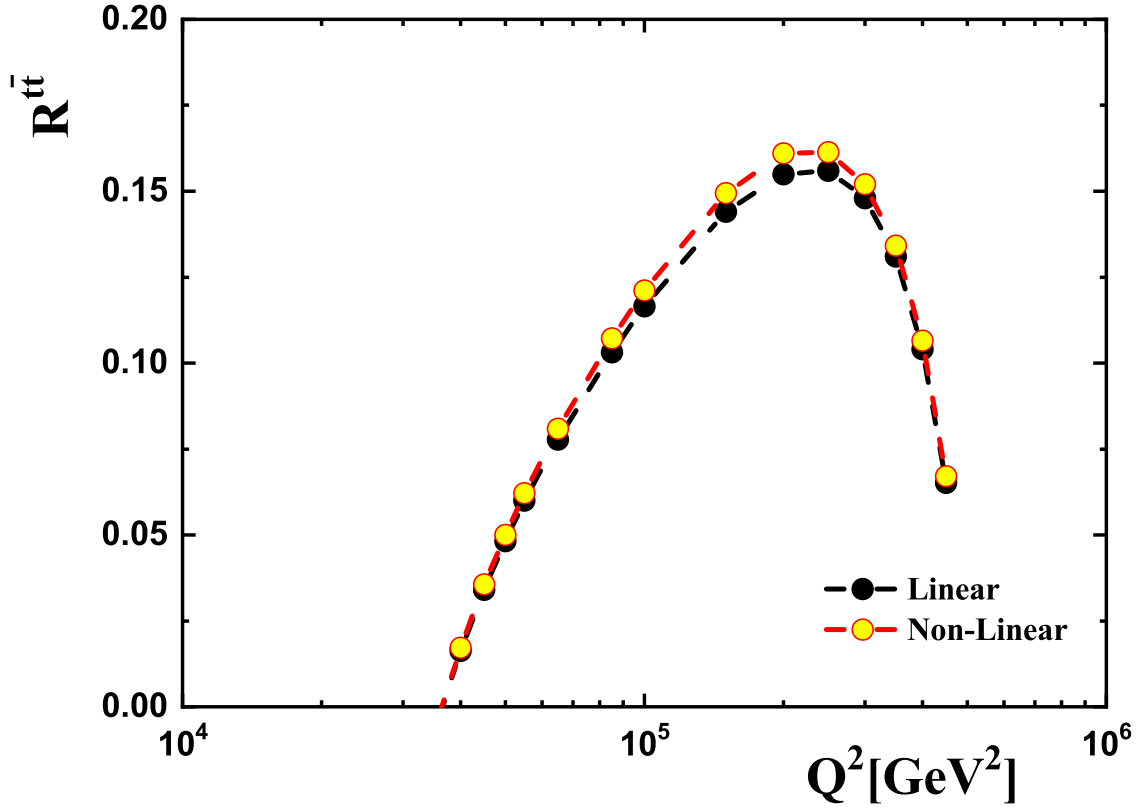


FIG. 3: The top contribution to the ratio  $R^{t\bar{t}}$  as a function of  $Q^2$  calculated at different  $x$  values at NNLO approximation. The non-linear corrections at hot-spot point are compared with linear in this figure.